

October 1999

COULOMB CRYSTALS AND GLASSES FOR SELF-ASSEMBLY OF NANOPARTICLES

P. F. Williams

University of Nebraska - Lincoln, pfw@moi.unl.edu

A. Belolipetski

University of Nebraska - Lincoln

A. Goussev

University of Nebraska - Lincoln

M. E. Markes

University of Nebraska - Kearney

Follow this and additional works at: <http://digitalcommons.unl.edu/elecengwilliams>



Part of the [Electrical and Computer Engineering Commons](#)

Williams, P. F.; Belolipetski, A.; Goussev, A.; and Markes, M. E., "COULOMB CRYSTALS AND GLASSES FOR SELF-ASSEMBLY OF NANOPARTICLES" (1999). *P. F. (Paul Frazer) Williams Publications*. 43.

<http://digitalcommons.unl.edu/elecengwilliams/43>

This Article is brought to you for free and open access by the Electrical & Computer Engineering, Department of at DigitalCommons@University of Nebraska - Lincoln. It has been accepted for inclusion in P. F. (Paul Frazer) Williams Publications by an authorized administrator of DigitalCommons@University of Nebraska - Lincoln.

Published in *Advanced Luminescent Materials and Quantum Confinement: Proceedings of the International Symposium Held in Honolulu, Hawaii on 18-20 October 1999*. Edited by Marc M. Cahay, S. Bandyopadhyay, D. J. Lockwood, N. Koshida, and J. P. Leburton.
Pennington NJ: The Electrochemical Society Inc., 1999.

Copyright © 1999 The Electrochemical Society Inc.

Used by permission.

COULOMB CRYSTALS AND GLASSES FOR SELF-ASSEMBLY OF NANOPARTICLES

P.F. Williams, A. Belolipetski, and A. Goussev
Department of Electrical Engineering
University of Nebraska-Lincoln
Lincoln, NE 68588-0511

M.E. Markes
Department of Physics
University of Nebraska-Kearney
Kearney, NE 68849

Abstract

Under proper conditions, small particles may be suspended in a regularly-spaced array called a Coulomb crystal. In this paper we discuss the application of this phenomenon to the self-assembly of nanoparticles in a lattice-like array on a substrate. Issues associated with depositing the particles, and the size and lattice spacing of the particles are discussed.

1 INTRODUCTION

There is interest in developing efficient and reliable technologies for synthesizing ordered arrays of ultrasmall structures such as quantum dots. These systems are potential vehicles for implementing a number of high performance electronic, magnetic and optical devices[1]. Dots small enough to host a single or few conduction electrons can be used for ultradense electronic or optical memory[2, 3, 4]. Cylindrical quantum dots of ferromagnetic materials have exhibited several-fold increase in magnetic coercivity accruing from shape anisotropy[5]. These dots could be used to create extremely high density magnetic storage disks. Recently, we have synthesized superconducting quantum dots of high T_c materials that have exhibited enhanced transition temperatures. Quantum dots of chemical catalysts are superior to their bulk counterparts since the surface-to-volume ratio increases dramatically. Additionally, self-assembled metallic dots can be utilized to fashion extremely powerful computing architectures[6] and they may have possible applications in such new and emerging areas as quantum computing[7]. In this paper, we will discuss a new technique for producing ordered or non-agglomerated arrays of small particles on a substrate.

It is well known that small particles in a plasma quickly acquire a negative charge. These particles can be levitated in a thin layer above electrodes and other surfaces exposed

to the plasma. Further, under proper conditions, these particles arrange themselves into a regularly-spaced array—a “Coulomb crystal.” This phenomenon can be used to produce a regimented distribution of these small particles which can be transferred to a substrate, resulting in self-assembly. Although the spatial coherence of these “crystals” can be good, generally spatial correlation falls off rapidly after several “lattice constants.” In this case, the structure might be better termed a “Coulomb glass.”

2 Use of Coulomb Crystals for Nano-Fabrication

The Coulomb crystal approach has a number of potential advantages over more established self-assembly techniques. First, it is much less expensive than Stranski-Krastanow growth which requires the use of an MBE apparatus or an equivalent facility. Second, unlike electrochemical self-assembly, it is a “dry” technique and hence compatible with hydrophobic materials. The material purity may not be as good as in the case of Stranski-Krastanow growth, but it is better than what is obtained in chemical self-assembly. Unlike S-K growth or electrochemical self-assembly, this technique has an advantage in that it offers the promise of continuously varying the period or pitch of the array by varying the plasma density. Finally, it is compatible with almost any type of substrate, and is more compatible with conventional IC fabrication technology than are other self-assembly techniques.

To self-assemble a two-dimensional ordered array of nanoparticles of a desired material on a chosen substrate, we follow a sequence of steps. First, the material must be formed into a fine powder. This can be accomplished by simply grinding it. While grinding damages the particles, for many applications the crystalline quality of the material is not of paramount importance. In many cases, the particles can be annealed or otherwise processed later to reduce the damage. Alternately, nanoparticles can be produced by gentler techniques such as sol-gel reactions or laser pyrolysis[8]. In fact, we have been investigating superconducting nanoparticles of high T_C materials produced by sol-gel reactions.

To arrange the nanoparticles on a substrate as a quasi-periodic array, we use an apparatus such as that shown schematically in Fig. 1. We first introduce them into an RF plasma by means of a “salt shaker”, which consists of a container with a porous membrane in the bottom. The container is shaken to sieve the particles into the plasma. This process provides a degree of particle size selection. The plasma occurs in an inert gas such as argon at a pressure typically of about 1 Torr. The R.F generator supplies about 10 W of power at 13.56 MHz through a standard matching network.

Once the particles are introduced into the plasma, they become negatively charged. The charged particles levitate in a quasi two-dimensional layer over the driven electrode in the plasma chamber because of Coulomb repulsion (the electrode is also negatively charged). Under proper conditions, the electrostatic interaction between the charged particles leads to the formation of a more-or-less regularly-spaced array of particles, a “Coulomb crystal” or “Coulomb glass.”. The array is then transferred to the substrate by simply turning the plasma off and allowing the particles to fall freely under gravity onto the substrate. We have found that spatial order is maintained reasonably well in this process. Several techniques can be used to stick the fallen particles to the substrate.

Considerable care is required to obtain good spatial coherence. Under many conditions, the particles form an array that would be better called a glass than a crystal. Even though

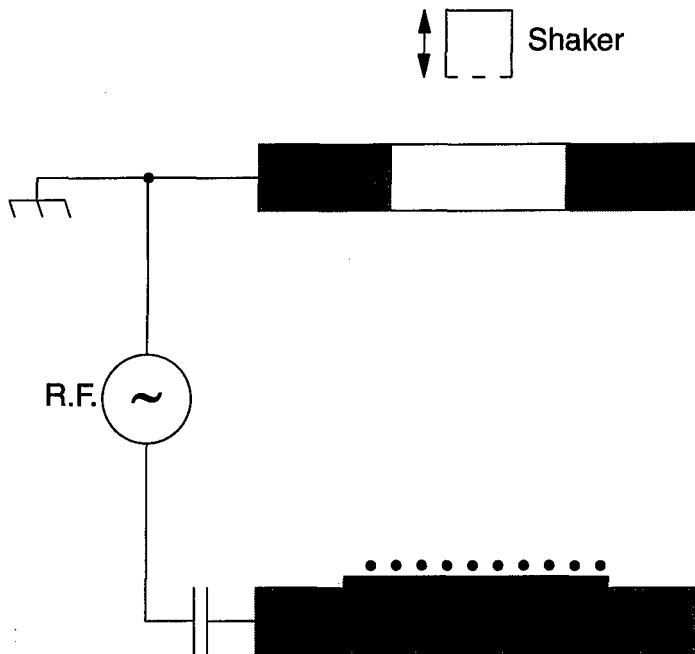


Figure 1: Schematic drawing of the cell used for deposition of regimented nanoparticle arrays.

they are not perfectly ordered, the particles in the glass are well-separated from each other and non-agglomerated. Such arrangements still exhibit interesting properties accruing from size quantization. For example, as discussed in a later section, we have recently synthesized Coulomb glasses of high T_C superconductors and found that they exhibit a somewhat enhanced transition temperature.

3 Physics of Coulomb Crystal Formation

It has been observed that small particles suspended in an R.F.-driven plasma will under the proper conditions collect in a quasi-two-dimensional layer just above the driven electrode, and arrange themselves into a regularly-spaced array—a so-called “Coulomb crystal.”[9] Similar structures have been seen in the positive column of glow discharges[10], thermal plasmas[11], ion traps[12], and even (originally) in colloidal suspensions[13]. It has been proposed that a Coulomb crystal could be produced by using photoionization to charge the particles[14], but to our knowledge, such a structure has not been demonstrated in the laboratory. The Coulomb crystal phenomenon has attracted considerable interest because of the insight it may lend into the formation and dynamics of conventional crystals, and because of possible technological applications.

Fig. 2 shows BCC and HCP crystals produced by Chu and I in a low pressure plasma[15]. These crystals are suspended in the plasma. The particle size is too large (several μm) for

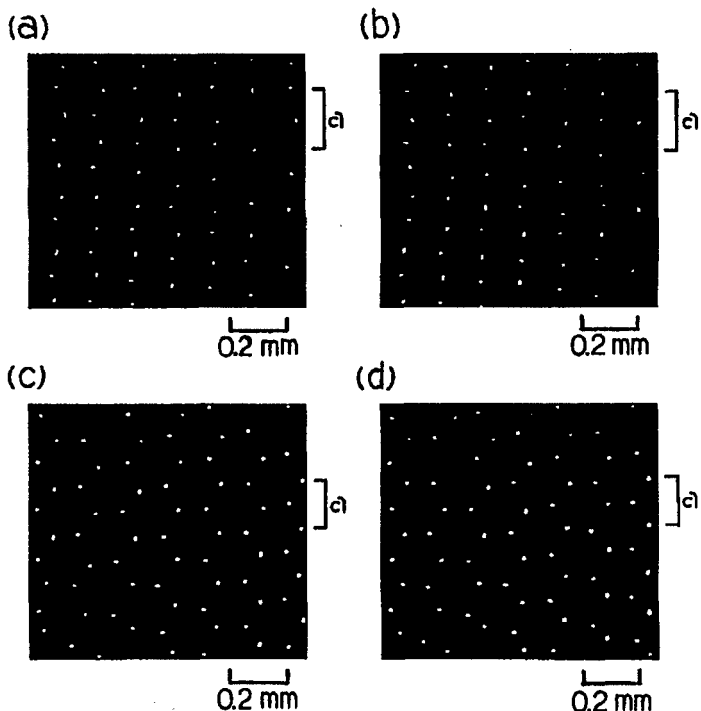


Figure 2: Micrographs of BCC (a and b) and HCP (c and d) Coulomb lattices from Ref. [15].

them to qualify as “quantum dots,” and the interparticle spacing is about $100 \mu\text{m}$. The particle diameter must be reduced by about two orders of magnitude, and it would be desirable to make a similar reduction in the interparticle spacing if this technique is to be useful for nanodevice applications. It appears that it is possible to reduce the particle diameter by the required amount, but substantial reduction of the interparticle spacing will be more difficult.

In most experiments (including ours), a low-pressure, parallel-plate, R.F. glow, two-component (free electrons and positive ions) plasma was used. Because the average speed of the electrons is much greater than that of the positive ions in the plasma, a particle in the plasma charges negatively. In steady state, the negative charge is adjusted so that the electron and positive ion currents balance. For a similar reason, the driven electrode of the plasma cell also charges negatively, causing a levitating force on particles in the vicinity. The combined effects of gravity, the ion wind, and this electric repulsion conspire to confine the particles to a thin sheet just above the electrode.

3.1 "Crystal" Bonding

According to the most common theory of Coulomb crystals, the particles levitated just above the driven electrode must be confined horizontally as well as vertically. The like-charged particles repel each other, and the lowest energy configuration is one with crystalline order. Thermal agitation of the particles acts to disrupt this order, and the system undergoes a phase transition similar to melting as this agitation is increased. The critical temperature depends on the parameter, Γ , defined as the ratio of the electrostatic energy of the particles at the equilibrium "lattice" position to the thermal translational energy of the particles. Values of Γ larger than about 170 are expected to result in formation of a regular lattice[16].

The interaction between the particles is complicated by the presence of the plasma. The negative charge on the particle repels the free electrons and attracts the positive ions, resulting in a halo of uncompensated ions around the particle. One effect of the halo is to shield the plasma from the field of the central particle. This effect is conventionally treated using a linearization of the Boltzmann distribution, resulting in Debye-Hückel shielding[17]. A second effect of the positive cloud is that it alters the effective force on a "dressed" particle when placed in a given electric field (such as that from a neighboring "dressed" particle). The net force is the vector sum of the force from the bare particle and the distorted positive cloud. The situation is roughly analogous to a classical diatomic molecule, and, over a range of particle separations, the net force between two "dressed" particles can be attractive, rather than repulsive. A rigorous calculation is difficult, however.

As a preliminary step in studying the process, we have calculated the net potential energy of a simplified two-"dressed" particle system as a function of particle separation. A principal simplification is that the force is treated as if the positive charge were rigidly attached to the negative particle. Thus, the net force on a particle is calculated as the sum of the force on the negative particle and the positive ion cloud. A second simplification relates to the electron and ion densities in the vicinity of the two particles. We have investigated several different approximations for this purpose. For all the situations we investigated, we found a net attraction between these "dressed" particles.

3.2 A Linear Model

The Debye-Hückel approximation for the electron and ion densities around a charged particle is obtained by 1) assuming thermodynamic equilibrium, so that the local densities are related to the local potential by a Boltzmann exponential, and 2) expanding the exponentials in a Taylor series and keeping only the linear terms. The result is that the local charge density, $\rho(\vec{r})$, is linearly related to the local potential, $\Phi(\vec{r})$, by

$$\rho(\vec{r}) = -\epsilon_0 \alpha^2 \Phi(\vec{r}) \quad (1)$$

where α has the dimensions of an inverse length, and is usually defined to be the reciprocal of the linearized Debye length, λ_D ,

$$\alpha = \frac{1}{\lambda_D} = \sqrt{\frac{n_0 q_e^2}{\epsilon_0} \left(\frac{1}{kT_i} + \frac{1}{kT_e} \right)} \quad (2)$$

Here, n_0 is the bulk plasma density, k the Boltzmann constant, and T_i and T_e are the ion and electron temperatures respectively, and q_e is the (unsigned) charge on an electron. Solving Poisson's equation for the case of an isolated particle of charge $-Zq_e$ gives

$$\Phi(\vec{r}) = \frac{-Zq_e e^{-\alpha r}}{\epsilon_0 r}$$

The case of two charged particles is handled relatively simply within this approximation. Because Eq. (1) is linear, the potential of two particles, one at the origin, and the other at \vec{R} , is simply the superposition of the potentials of the isolated particles.

The interaction energy may be evaluated as

$$U = \frac{1}{2} \int \rho(\vec{r}) \Phi(\vec{r}) d^3 r. \quad (3)$$

Eq. (3) can be evaluated exactly for the case of two particles separated by a distance, R , giving

$$U(R) = U_0 \left(\frac{\lambda_D}{R} - \frac{1}{2} \right) e^{-R/\lambda_D} \quad (4)$$

where $U_0 = Z^2 q_e^2 / 4\pi\epsilon_0 \lambda_D$ is the energy of two unshielded particles separated a distance λ_D . Fig. (3) shows a plot of $U(R)/U_0$ vs. R/λ_D . There is a potential well of depth $0.00872U_0$, located at $R = (1 + \sqrt{3})\lambda_D \approx 2.73\lambda_D$.

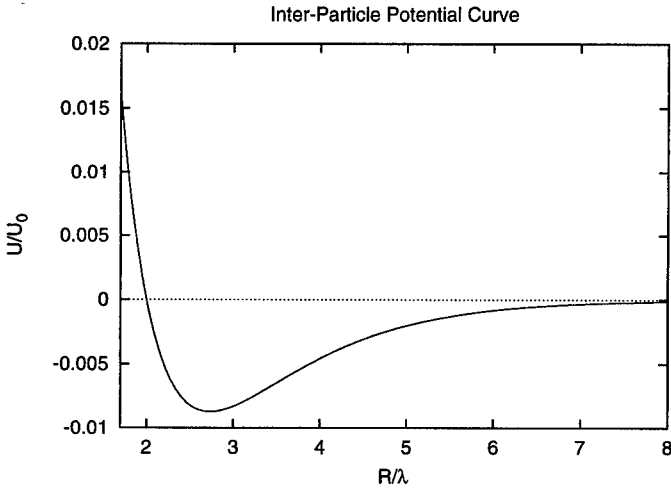


Figure 3: Inter-particle potential energy curve. The units of energy are $Z^2 q_e^2 / 4\pi\epsilon_0 \lambda_D$, the energy of two unshielded particles separated a distance λ_D .

The assumption that the ion density is given by a linearized Maxwellian distribution is questionable in this application. Because of recombination at the dust particles, the ions are not in thermodynamic equilibrium, and even if equilibrium prevailed the exclusion of second order and higher terms in the expansion of the Maxwellian is typically not justified. Daugherty *et al.*[18], however, have shown that a linear relation such as that in Eq. (1) provides a remarkably good approximation to the results they obtain from a presumably more accurate theory similar to that conventionally used to analyze spherical Langmuir probes. Perhaps the Debye-Hückel-like approximation works as well as it does because the two errors (non-equilibrium, and linearization) partly cancel.

3.3 A Collisionless Model

A rather different model is also tractable. In this model, the electron density around the particle is assumed to be given by a Boltzmann distribution, and the positive ion density is determined by tracking ion trajectories as they pass by the particle, assuming that there are no collisions. The ion density, $n_+(\vec{r})$, at a point inside the sheath is given by

$$n_+(\vec{r}) = \int f_+(\vec{r}, \vec{v}) d^3v \quad (5)$$

where $f_+(\vec{r}, \vec{v})$ is the ion distribution function. Watson showed that for a collisionless ensemble[19, 20]

$$f_+(\vec{r}, \vec{v}) = f(\vec{r}_0, \vec{v}_0) \quad (6)$$

where (\vec{r}_0, \vec{v}_0) is any point which is on the same trajectory as the point (\vec{r}, \vec{v}) .

We assume that the particles are located within a collisionless sheath of radius r_0 , outside of which the ions are in local thermodynamic equilibrium. Then f_+ is a Maxwellian distribution on the surface of the sheath region. Other treatments assume monoenergetic ions at the sheath edge[18]. The assumption apparently is made for convenience, but the results are not significantly simpler than those we obtain. Eqs. (5) and (6) may be combined to obtain

$$n_+(\vec{r}) = n_0 \left[\frac{2}{\pi} \sqrt{-q_e \Phi(\vec{r})/kT} + \operatorname{erfc} \left(\sqrt{-q_e \Phi(\vec{r})/kT} \right) e^{-q_e \Phi(\vec{r})/kT} \right] \quad (7)$$

In deriving these results, closed orbits and ion collisions with the particle are neglected.

This result can be used in Poisson's equation to determine Φ . Doing so produces a non-linear differential equation that can be solved numerically. The inter-particle potential can then be calculated numerically from Eq. (3) using this result for Φ along with n_+ from Eq. (7), and n_e from a Boltzmann distribution. Fig. (4) shows the results obtained for 2 μm diameter particles, $Z = 1000$, $n_0 = 10^9 \text{ cm}^{-3}$, and $T_e = 1$ and $T_i = 0.026 \text{ eV}$. Also shown for comparison are the results of the linearized Debye-Hückel model under the same conditions.

In these calculations, the charge density was taken to be the superposition of the densities of the isolated particles. Since the relationship between charge density and potential is not linear, this procedure is an approximation. The positive ion clouds will surely distort as the two "dressed" particles are brought together—an effect that we have tacitly neglected in the Langmuir-like model, and absent in the linearized model. The important point here is that such a distortion will cause the ion distribution to relax to a *lower-energy* configuration than that of the fixed configuration we used. Thus, we will have under-estimated the attractive force, and a more sophisticated treatment would find a stronger attraction than we find. The qualitative conclusion that the net force is attractive is still correct.

3.4 Empirical Evidence

The existence of an attractive force has been verified experimentally by Chen *et al.*[21] They present photographs of dust particles in a parallel-plate RF discharge showing "molecules" of six particles in hexagonal and square configurations. They also show a photograph which seems to show several "diatomic" and "triatomic" molecules, but the interpretation of these data is complicated by the possibility that the photo may be showing two or more

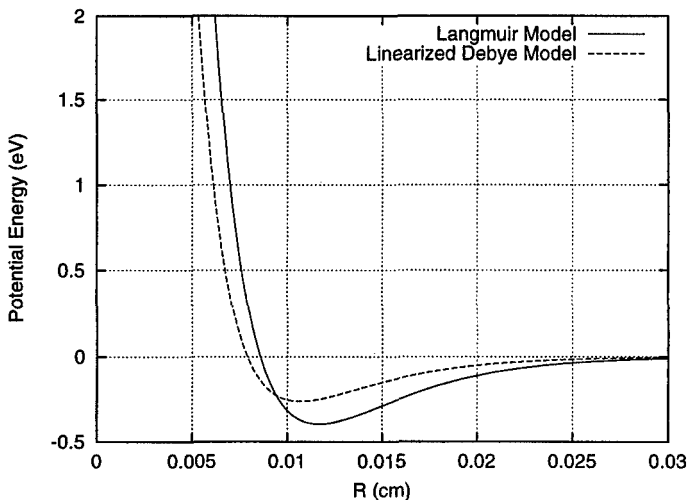


Figure 4: Comparison of the inter-particle potential energy obtained from the Langmuir-like and Debye-Hückel models. The assumed particle diameter was $2 \mu\text{m}$, $Z = 1000$, $n_0 = 10^9 \text{ cm}^{-3}$, $T_e = 1 \text{ eV}$, and $T_i = 0.026 \text{ eV}$.

layers of a Coulomb crystal. The existence of isolated “molecules” provides substantial empirical support for the claim that the inter-particle force is attractive. Additionally, several workers report that the individual particles in adjacent layers line up so that a particle in one layer is directly above the corresponding particle in the layer just below [22, 23]. This observation also supports the attractive force contention.

4 ISSUES FOR NANOFABRICATION

Several problems should be solved in order that this technique be considered viable for nanofabrication applications. Among these are

1. Transfer of the particle array from plasma to substrate.
2. Reduction in particle size to “nano” dimensions.
3. Reduction in inter-particle spacing values less than $1 \mu\text{m}$.

Of these the first two are the most important, and, fortunately, these seem well in hand. Although the third problem will be more difficult to solve, an adequate solution is required only for some applications.

4.1 Deposition on the Substrate

After the Coulomb crystal has formed, it must be transferred to a substrate without excessively disturbing the long range order. Transfer can be accomplished in the standard

configuration by simply turning off the plasma and letting the particles fall to the surface. If the particles do not adhere adequately to the surface, they can be "glued" to the surface by coating the surface with a viscous material, or by depositing a suitable thin film over them. Deposited particles can also be used as a mask for a sputtering or reactive-ion etching process carried out *in situ* to create mesa-etched or buried quantum dots in a suitable substrate. For example, Lim *et al.* have demonstrated the creation of 9 nm pillars in silicon using Au clusters as an etching mask[24]. Alternately, if the composition of the particles allows it, the surface can be heated to make the particles react chemically with or diffuse into the surface. Doing so will undoubtedly degrade the size control, but it may still be *within tolerable limits for many applications.*

We have produced non-agglomerated arrays of particles on a substrate by using a "glue." The construction of the cell (see Fig. 1) is such that the driven electrode is near the bottom, and that the plasma forms above it. The substrate is coated with a suitable sticky substance (partially cured G.E. varnish seems to work well for this purpose) and placed on top of the driven electrode. When the R.F. power is abruptly turned off the particles fall 1–2 mm onto the substrate. The "glue" holds them in place sufficiently well that the substrate can be removed from the chamber, and a more robust fixing method applied to permanently fix them in place.

Besides disorder introduced as the particles fall onto the substrate, the existence of multiple layers in the Coulomb crystal introduces another potential problem. Typically, there are several layers each containing a regimented array, and each layer will fall onto the substrate. If the layers are not well correlated, this will be a second source of disorder in the deposited array. It is found that the layers tend to align themselves such that particles in one layer are directly above the corresponding particle in the layer just below[22, 23]. Because we have looked mostly at Coulomb glasses, we do not have very good information about the effect of multiple layers on the ordering of the deposited particles. Certainly, for good order it would be desirable to employ a technique producing only one layer.

4.2 Particle Size

For most applications particle diameter is a critical parameter. Particle spacing is also relevant, but in many cases it is not critical. In published experiments, particle diameters have typically been 1 to 10 μm . In order for this technique to be applicable to nanoscale structures, the particle diameter must be reduced by more than an order of magnitude, to ≈ 100 nm. It appears that the required reduction in particle size should not be difficult. With no special effort, we have formed Coulomb glasses of 300 nm diameter alumina particles, and Boufendi *et al.* report observing strongly coupled particles of about 250 nm diameter in a processing plasma[25].

4.3 Particle Spacing

For many applications, it is desirable to reduce the spacing between particles to a value less than 1 μm . This goal may be more difficult to achieve. The interparticle forces responsible for the bonding of particles to form crystalline structures is not well understood. In most theories, the interparticle spacing is closely related to the Debye length in the plasma,

$$\lambda_D = \left[\frac{q_e^2 n_0}{k\epsilon_0} \left(\frac{1}{T_e} + \frac{1}{T_i} \right) \right]^{-1/2}$$

where T_e and T_i are the electron and ion temperatures, and n_0 is the plasma density. For a typical, low-power, parallel-plate, R.F. discharge, $n_0 \approx 10^9 \text{ cm}^{-3}$, $T_e \approx 2 \text{ eV}$, and $T_i \approx 0.025 \text{ eV}$, leading to $\lambda_D \approx 40 \mu\text{m}$. The inter-particle spacing in the Coulomb crystals described to date are typically a few times this value.

According to the standard theory of Coulomb crystals, crystallization depends on the parameter Γ , defined as the ratio of the electrostatic energy (Φ) to the thermal translational energy of the particles ($k_B T$). Values of Γ larger than roughly 170 are expected to result in formation of a regular lattice[16]. For a given set of parameters, Φ would be expected to decrease with particle diameter because of reduced charge, and to increase with decreasing lattice constant because of reduced inter-particle separation.

The principal conclusion from our models is that there is a potential minimum. The lattice constant of a Coulomb crystal would be determined by the location of this minimum, and is predicted to be a few times the Debye length. This prediction is consistent with the lattice spacing observed empirically. Theories based on electrostatic repulsion between trapped, charged particles make a similar prediction. The Debye length, λ_D , in turn, is inversely proportional to the square root of the plasma density. For typical parameters in a parallel-plate, capacitive R.F. discharge, the plasma density is 10^9 cm^{-3} , and $\lambda_D \approx 40 \mu\text{m}$. To obtain smaller lattice constants higher plasma densities are required. We find qualitative verification of this prediction in our experiments. As we increase the R.F. power the particle separation decreases, and *vice versa*. Quantitative measurements are difficult, however, because the relation between R.F. power and plasma density is not simple, and increasing the power also changes other plasma parameters, such as electron temperature.

Continuing along these lines, it appears that to obtain a lattice constant of $1 \mu\text{m}$, a plasma density of about 10^{12} cm^{-3} will be required. The upper limit for plasma density in parallel plate reactors is probably about 10^{10} cm^{-3} . Fortunately, there exist other configurations capable of producing densities up to about 10^{13} cm^{-3} . Inductively-coupled plasmas such as barrel and TCP reactors routinely produce densities of 10^{12} cm^{-3} [26], and wave-heated discharges such as ECR and helicon discharges can produce plasma densities up to 10^{14} cm^{-3} [27]. Surface wave discharges routinely produce plasma densities above 10^{11} cm^{-3} , and 10^{15} cm^{-3} has been reported[28]. The neutral density in these high-plasma-density discharges is typically lower (10 mTorr vs. 1 Torr) than in parallel-plate reactors and the neutral temperature is higher ($100^\circ\text{--}200^\circ$ vs. 30°C). The higher temperature and lower neutral density may lead to more disordered lattices, but on the other hand the potential energy minimum becomes narrower and deeper as the plasma density increases, which would lead to a more ordered array. Thus, it is not clear *a priori* whether these high-density plasmas will be conducive or detrimental to better ordering.

Kunhardt has reported achieving electron densities of the order of 10^{12} cm^{-3} in an atmospheric-pressure helium discharge[29]. In these discharges a relatively high plasma density is achieved while maintaining a neutral temperature near room temperature. Schoenbach *et al.*[30] and Frame *et al.*[31], also report glow-like discharges in near-atmospheric pressure gases using a somewhat different configuration, but do not report plasma density or neutral temperature. These high-neutral-density discharges appear promising for production of Coulomb crystals. The low neutral temperature, coupled with the high pressure should provide good cooling of the particles, while the high plasma density should provide reduced lattice constant.

5 AN APPLICATION— T_C ENHANCEMENT

The critical temperature, T_C , of a superconductor depends on the electronic density of states. In nanoparticles this density of states can be modified substantially over the bulk form because of wavefunction confinement, with the density becoming peaked around discrete energy values. One effect of this change should be an increase in T_C , relative to bulk material.

In order to test this hypothesis, we have synthesized Coulomb glasses of YBCO with particle diameter less than about 300 nm and transferred them to a silicon substrate. GE varnish was used as the "glue" to stick the particles to the substrate. To our knowledge, this is the first time that a Coulomb glass (or crystal) of a high T_C superconductor has been produced and transferred intact to a substrate. SQUID measurements were carried out to determine the transition temperature T_C in these YBCO quantum dots. The T_C of samples was increased by up to 4–6 K.

6 ACKNOWLEDGEMENTS

We thank J. Betanabhatla for providing us with the YBCO starting material for the T_C experiments, and L. Menon and S. Bandyopadhyay for making the measurements of T_C . We acknowledge helpful conversations with S. Bandyopadhyay, E.E. Kunhardt, and M.J. Kushner. The work was supported by the Nebraska Research Initiative.

References

- [1] D. S. Chemla, D. A. B. Miller, and P. W. Smith, in R. Dingle, ed., *Semiconductors and Semimetals* (Academic Press, 1987), pp. 279–318.
- [2] A. J. Shields, M. O'Sullivan, I. Farrer, D. Ritchie, K. Cooper, C. Foden, and M. Pepper, *Appl. Phys. Lett.* **74**, 735 (1999).
- [3] S. Tiwari, F. Rana, H. Hanafi, A. Hartstein, E. F. Crabbè, and K. Chan, *Appl. Phys. Lett.* **68**, 1377 (1996).
- [4] L. Zhuang, L. Guo, and S. Y. Chou, *Appl. Phys. Lett.* **72**, 1205 (1998).
- [5] S. Bandyopadhyay, L. Menon, N. Kouklin, H. Zheng, and D. J. Sellmyer, *J. Elec. Mat.*: Special Issue on Quantum Dots In Press.
- [6] V. P. Roychowdhury, D. B. Janes, and S. Bandyopadhyay, *Proc. IEEE* **85**, 574 (1997), and references therein.
- [7] S. Bandyopadhyay, A. Balandin, V. Roychowdhury, and F. Vatan, *Superlat. Microstruct.* **23**, 445 (1998).
- [8] E. Barsella, S. Botti, M. Cremona, S. Martelli, R. Montereali, and A. Nesterenko, *J. Mat. Sci. Lett.* **16**, 221 (1997).
- [9] G. Morfill and H. Thomas, *J. Vac. Sci. Technol. A* **14**, 490 (1996).

- [10] V. Fortov, A. Nefedov, V. Torchinskii, V. Molotkov, A. Khrapak, O. Petrov, and K. Volykhin, *JETP Lett.* **64**, 92 (1996), [*Pis'ma Zh. Èksp. Teor. Fiz.* **64**, 86-91 (1996)].
- [11] V. Fortov, A. Nefedov, O. Petrov, A. Samarian, A. Chernyshev, and A. Lipaev, *JETP Lett.* **63**, 187 (1996), [*Pis'ma Zh. Èksp. Teor. Fiz.* **63**, 176-180 (1996)].
- [12] I. Waki, S. Kassner, G. Birkl, and H. Walther, *Phys. Rev. Lett.* **68**, 2007 (1992).
- [13] C. Murray and D. V. Winkle, *Phys. Rev. Lett.* **58**, 1200 (1987).
- [14] M. Rosenberg and D. Mendis, *IEEE Trans. Plasma Sci.* **23**, 177 (1995).
- [15] J. Chu and L. I, *Physica A* **205**, 183 (1994).
- [16] H. Ikezi, *Phys. Fluids* **29**, 1764 (1986).
- [17] M. Lieberman and A. Lichtenberg, *Principles of Plasma Discharges and Materials Processing* (Wiley, 1994), pp. 40-42.
- [18] J. Daugherty, R. Porteous, M. Kilgore, and D. Graves, *J. Appl. Phys.* **72**, 3934 (1992).
- [19] K. Watson, *Phys. Rev.* **102**, 12 (1956).
- [20] K. Brueckner and K. Watson, *Phys. Rev.* **102**, 19 (1956).
- [21] Y.-P. Chen, H. Luo, M.-F. Ye, and M. Yu, *Phys. of Plasmas* **6**, 699 (1999).
- [22] Y. Hayashi and K. Tachibana, *Jpn. J. Appl. Phys.* **33**, L804 (1994).
- [23] J. Pieper, J. Goree, and R. Quinn, *J. Vac. Sci. Technol. A* **14**, 519 (1996).
- [24] S. Lim, Y. Shimogaki, Y. Nakano, K. Tada, and H. Komiyama, *Appl. Phys. Lett.* **68**, 832 (1996).
- [25] L. Boufendi, A. Bouchoule, R. Porteous, J. P. Blondeau, A. Plain, and C. Laure, *J. Appl. Phys.* **73**, 2160 (1993).
- [26] M. Lieberman and A. Lichtenberg, *Principles of Plasma Discharges and Materials Processing* (Wiley, 1994), p. 388.
- [27] M. Lieberman and A. Lichtenberg, *Principles of Plasma Discharges and Materials Processing* (Wiley, 1994), p. 434.
- [28] J. Margot and M. Moisan, in P. Williams, ed., *Plasma Processing of Semiconductors* (Kluwer, 1996), pp. 187-210.
- [29] E. Kunhardt, Unpublished (1998).
- [30] K. Schoenbach, R. Verhappen, T. Tessnow, F. Peterkin, and W. Byszewski, *Appl. Phys. Lett.* **68**, 13 (1996).
- [31] J. Frame, D. Wheeler, T. DeTemple, and J. Eden, *Appl. Phys. Lett.* **71**, 1165 (1997).